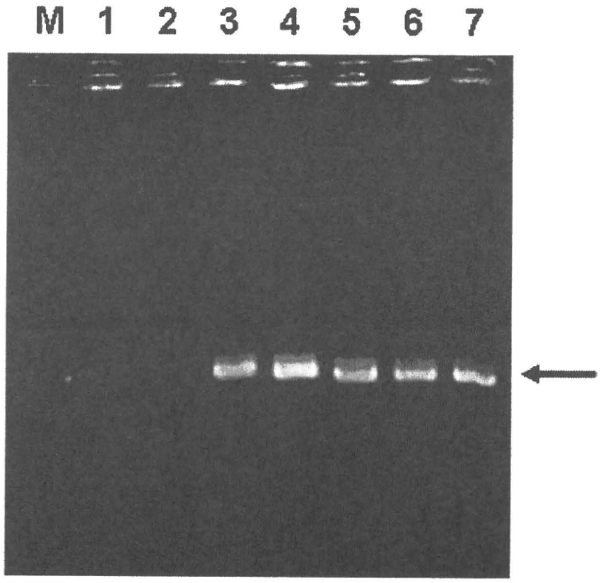

Supplementary Figure 1. Presence of *COL/EGFP* transgene in the recipients' spleen tissues. Spleen tissues were excised from COL/EGFP-recipient mice. They were subjected to DNA isolation and subsequent polymerase chain reaction (PCR) analyses to detect the presence of *COL/EGFP* transgene (*arrows* in *lanes 3–7*). Spleen DNA obtained from the wild-type C57BL/6 mice was also included as a negative control (*lanes 1* and *2*). Further analyses using real-time PCR assays of *COL/EGFP* transgene and *glyceraldehyde 3-phosphate dehydrogenase* gene as a control determined the chimerism of *COL/EGFP*-positive cells in the spleen tissue. Presence of *COL/LUC* transgene was detected in the same manner. *M*, DNA size markers.

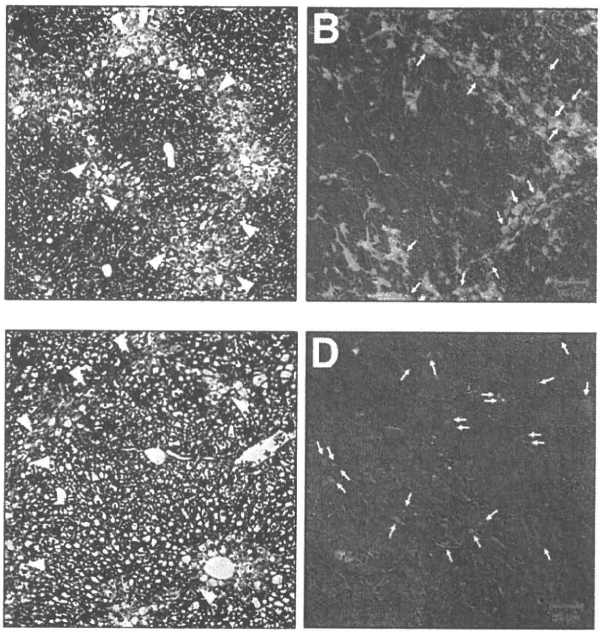

Supplementary Figure 2. Activation of *COL1A2* promoter at an early stage of liver fibrosis. Transgenic COL/EGFP mice (*A* and *B*) or their BM recipients (*C* and *D*) were treated with repeated CCl_4 injections every 3 days for a total of 10 times. Liver specimens were obtained 48 hours after the last CCl_4 injection and subjected to Azan–Mallory staining (*A* and *C*) or confocal laser-scanning microscopic examination (*B* and *D*). Representative pictures are shown from 3 to 4 mice in each group. Azan–Mallory staining indicated the histopathologic features of an early stage of liver fibrosis with thin fibril formation (*arrowheads*) and fatty degeneration. EGFP expression was detected in a large number of mesenchymal cells in liver tissues obtained from COL/EGFP mice (*green* in *B*) but not in those from their BM recipients (*D*). Note that the pale signals (*arrows*) observed in both *panels B* and *D* represent nonspecific autofluorescence but not the specific EGFP signals. Original magnification, 40× in *A* and *C*. *Scale bars*, 50 μm in *B* and *D*.

Hepatology Research

Hepatology Research 2010; 40: 853–861 doi: 10.1111/j.1872-034X.2010.00687.x

Original Article

Usefulness of transient elastography for assessment of liver fibrosis in chronic hepatitis B: Regression of liver stiffness during entecavir therapy

Masaru Enomoto,[1] Mami Mori,[1] Tomohiro Ogawa,[1] Hideki Fujii,[1] Sawako Kobayashi,[1] Shuji Iwai,[1] Hiroyasu Morikawa,[1] Akihiro Tamori,[1] Hiroki Sakaguchi,[1] Ayumi Sawada,[2] Setsuko Takeda,[2] Daiki Habu,[3] Susumu Shiomi[4] and Norifumi Kawada[1]

[1]Department of Hepatology, Osaka City University Graduate School of Medicine, [2]Central Clinical Laboratory, Osaka City University Medical School Hospital, [3]Department of Medical Nutrition, Osaka City University Graduate School of Life Science, and [4]Department of Nuclear Medicine, Osaka City University Graduate School of Medicine, Osaka, Japan

Aim: The usefulness of transient elastography remains to be validated in chronic hepatitis B, particularly as a tool for monitoring the degree of liver fibrosis during treatment.

Methods: The subjects were 50 patients with chronic hepatitis B virus infection. Liver biopsy was performed in 38 patients, and in 12 patients with platelet counts of 50×10^9/L or less, cirrhosis was clinically diagnosed on the basis of specific signs of portal hypertension. Liver stiffness was measured by transient elastography at baseline and after 12 months of treatment in 20 nucleos(t)ide-naïve patients who started entecavir within 3 months after study entry.

Results: Twenty (40%) patients were classified as F1, 10 (20%) as F2, 5 (10%) as F3, and 15 (30%) as F4 (cirrhosis). Median liver stiffness (interquartile range) was 7.0 kPa (5.6–9.4), 9.8 kPa (5.6–14.7), 9.8 kPa (7.6–12.9), and 17.3 kPa (8.2–27.6) in fibrosis stages F1 to F4, respectively. Liver stiffness significantly correlated with fibrosis stage ($r = 0.46$; $P = 0.0014$). Of the patients who started entecavir, median liver stiffness significantly decreased from 11.2 kPa (7.0–15.2) to 7.8 kPa (5.1–11.9; $P = 0.0090$) during 12 months of treatment. Median levels of amino-terminal peptide of type III procollagen and type IV collagen 7S domain in serum significantly decreased from 0.9 (0.6–1.3) to 0.6 (0.5–0.7) U/mL ($P = 0.0010$) and from 5.0 (4.4–6.7) to 3.9 (3.2–4.4) ng/mL ($P = 0.015$), respectively.

Conclusion: Liver stiffness measurement can be useful for monitoring regression of liver fibrosis during entecavir treatment in patients with chronic hepatitis B virus infection.

Key words: chronic hepatitis B virus, entecavir, FibroScan, liver stiffness, transient elastography.

INTRODUCTION

INFECTION WITH HEPATITIS B virus (HBV) remains an important public health problem and a leading cause of liver-related morbidity worldwide.[1] Currently available antiviral therapy for chronic HBV includes the immunomodulator interferon and oral nucleos(t)ide analogues.[2,3] Entecavir, a cyclopentyl guanosine analogue, is the most potent agent against HBV among licensed nucleos(t)ide analogues and is used as the first-line treatment of choice for chronic HBV infection. Randomized controlled trials have demonstrated not only virological and biochemical responses, but also a histological response (defined as 2-point reduction in the Knodell necroinflammatory score without progression to fibrosis) in patients treated with entecavir.[4,5] A *post hoc* descriptive analysis of the trials showed that the stage of fibrosis was improved in 58% of nucleos(t)ide-naïve patients with advanced liver fibrosis by 52 weeks of entecavir treatment.[6]

Liver biopsy is considered the gold standard for diagnosing chronic liver disease, grading necroinflammatory activity, and staging liver fibrosis. However, sampling error can lead to underestimation of the degree of liver fibrosis, especially when biopsy specimens are small or fragmented. In addition, interpretation of the results is subject to significant intra- and inter-observer

Correspondence: Professor Norifumi Kawada, Department of Hepatology, Osaka City University Graduate School of Medicine, 1-4-3 Asahimachi, Abeno-ku, Osaka 545-8585, Japan. Email: kawadanori@med.osaka-cu.ac.jp

Received 18 January 2010; revision 27 April 2010; accepted 3 May 2010.

variability. Moreover, liver biopsy is not suitable for repeated evaluations, because it is invasive and can cause major complications (0.3–0.5%), including death (0.03–0.1%).[7,8] Several surrogate serum markers and laboratory indices/scores thus have been proposed as alternative techniques for the non-invasive assessment of liver fibrosis.[9,10] More recently, transient elastography (FibroScan; Echosens, Paris) has been introduced and found to be a rapid, objective, and promising technique for staging liver fibrosis by measuring liver stiffness.[11,12] In a meta-analysis of 50 studies done mainly in chronic hepatitis C, the mean areas under the receiver operating characteristic curve for the diagnosis of significant fibrosis, severe fibrosis, and cirrhosis were 0.84, 0.89, and 0.94, respectively.[13]

Compared to hepatitis C virus, the usefulness of transient elastography has been less extensively studied and validated in chronic HBV. In particular, transient elastography has not been evaluated as a tool for monitoring regression of liver fibrosis during antiviral treatment for chronic HBV, although patients' acceptance of repeated evaluations is excellent.

The aim of this study was to determine whether liver stiffness as measured by transient elastography can be used for on-treatment monitoring of the effects of entecavir on liver fibrosis in patients with chronic HBV. First, we evaluated the correlation between liver stiffness and the stage of fibrosis in 50 patients with chronic HBV. Second, in 20 patients who started entecavir within 3 months after study entry, liver stiffness, as well as serum levels of liver fibrosis markers, was measured at baseline and after 12 months of treatment.

METHODS

Patients

THE FLOW OF the participants through the trial is shown in Figure 1. Between April 2005 and June 2008, 38 patients with chronic HBV in whom liver biopsy was clinically indicated were admitted to our hospital. During the same period, 12 other patients with chronic HBV in whom percutaneous liver biopsy was contraindicated by a low platelet count ($\leq 50 \times 10^9$/L) received a clinical diagnosis of cirrhosis on the basis of specific signs of portal hypertension, such as esophageal varices.

A total of 50 consecutive patients with chronic HBV were included in this study. We excluded patients who had antibodies to hepatitis C virus and other likely causes of chronic liver diseases; ascites and other clinical signs of decompensated liver disease; acute exacerbations of liver disease, defined as a rise in alanine aminotransferase (ALT) to 10-times higher than the upper limit of normal; or hepatocellular carcinoma detectable by ultrasonography in the target area for liver stiffness measurement. Informed consent was obtained from each patient. The procedures of the study were in accordance with the Helsinki Declaration of 1975 (2000 revision).

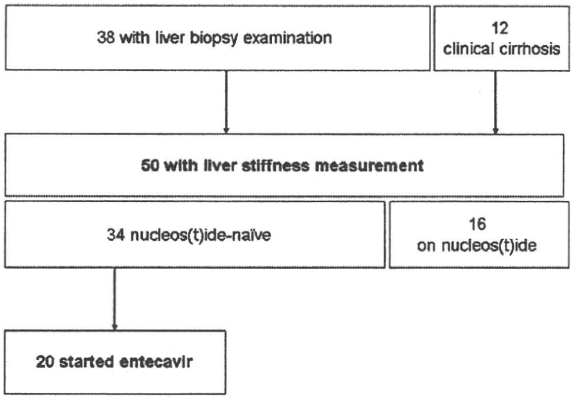

Figure 1 Flow of participants through the trial. Of the 50 patients studied, 16 were receiving nucleos(t)ide analogue treatment at entry. Of the remaining 34 nucleos(t)ide-naïve patients, 20 patients started entecavir within 3 months of entry.

Liver histology and quantification of liver fibrosis

Liver biopsies were performed with a 15-gauge Tru-Cut needle (Hakko, Tokyo) under ultrasound guidance. Liver tissues were fixed in formalin immediately after biopsy and embedded in paraffin. Four-micrometre-thick sections were stained with hematoxylin-eosin and Sirius red and immunostained with α-smooth muscle actin (Dako, Glostrup). The stage of liver fibrosis and grade of necroinflammatory activity were evaluated semiquantitatively according to the METAVIR scoring system as follows: F1, portal fibrosis without septa; F2, portal fibrosis and few septa; F3, numerous septa without cirrhosis; and F4, cirrhosis.[14] METAVIR activity scores were defined as follows: A1, mild; A2, moderate; and A3, severe. A liver sample was considered adequate if it was longer than 15 mm and contained six or more portal tracts.

In some biopsy specimens, morphometric image analysis was performed with a computerized system, consisting of a photomicroscope, digital camera, and

LuminaVision 2.4 bio-imaging software (Mitani, Tokyo), to quantitatively assess fibrosis. The proportion of area stained with Sirius red or α-smooth muscle actin in liver-biopsy sections was calculated as the sum of the pixel-wise bound stain measurements divided by the number of summed pixels.

Liver stiffness measurement

Liver stiffness was measured by transient elastography (FibroScan; EchoSens)[11,12] within 3 months of study entry. Briefly, this system is equipped with a probe including an ultrasonic transducer mounted on the axis of a vibrator. The subject laid down on a bed in the horizontal supine position with the right arm in maximal abduction, and a probe was placed on the skin above the right intercostal space. A vibration transmitted from the vibrator toward the tissue induces an elastic shear wave that propagates through the right lobe of the liver. These propagations are followed by pulse-echo ultrasound acquisitions, and their velocity, which is directly related to tissue stiffness, is measured. The median of ten successful measurements was expressed in units of kilopascals (kPa) and used as the liver stiffness for a given subject. Performance was considered optimal when the rate of successful measurements to the total number of acquisitions was at least 60% and the ratio of the interquartile range to the median value did not exceed 30%.

Biochemical, hematological, and virological examinations

The following variables were determined at baseline: serum ALT activity, platelet count, HBV surface antigen, HBV e antigen (HBeAg), anti-HBe, HBV genotypes, and HBV DNA levels. HBV surface antigen, HBeAg, and anti-HBe were detected by chemiluminescence enzyme immunoassay. Genotypes of HBV were identified by enzyme-linked immunosorbent assay (Institute of Immunology, Tokyo).[15] HBV DNA was measured by transcription-mediated amplification with a hybridization protection assay (Chugai Diagnostics, Tokyo); the detection range was 3.7–8.7 $\log_{10}$ copies/mL.[16] If HBV DNA was not detected by this method, a PCR-based Amplicor Monitor test (Roche Molecular Systems, Pleasanton, CA) was utilized; the detection range was 2.6–7.6 $\log_{10}$ copies/mL.[17]

Surrogate serum markers of liver fibrosis

In patients who started entecavir within 3 months of entry, two serum markers of liver fibrosis were measured at baseline and after 12 months of treatment. Serum levels of amino-terminal peptide of type III procollagen (PIIINP) were measured by radioimmunoassay (Nihon Schering K.K., Osaka), with a normal range of 0.3–0.8 U/mL. Serum levels of type IV collagen 7S were measured by radioimmunoassay (Mitsubishi Kagaku Iatron, Tokyo), with a normal range of not more than 6 ng/mL.

Statistical analysis

Statistical analysis was performed with the Statview SE + Graphics program, version 5.0 (SAS Institute, Cary, NC). Distributions of continuous variables were analyzed by the Mann–Whitney *U*-test. Differences in proportions were evaluated by Fisher's exact test. The significance of correlation was tested by Spearman's rank analysis. The significance of changes in values between two time points was evaluated by the Wilcoxon signed-rank test. A two-tailed *P*-value of less than 0.05 was considered to indicate statistical significance.

RESULTS

Baseline characteristics of patients

TABLE 1 SHOWS the baseline characteristics of the enrolled patients with chronic HBV. Mean body mass index was 22.4 kg/m^2; six patients were overweight (25–30 kg/m^2), and no patient was obese (>30 kg/m^2). Among all 50 subjects, 16 were receiving nucleos(t)ide analogue treatment at entry: 5 were receiving lamivudine, 2 lamivudine plus adefovir dipivoxil, and 9 entecavir (Fig. 1). Among the remaining 34 nucleos(t)ide-naïve patients, 20 started entecavir at an oral dose of 0.5 mg once daily within 3 months after entry. The 20 patients who started entecavir had significantly higher ALT ($P = 0.018$) and HBV DNA levels ($P = 0.011$) and a lower stage of fibrosis ($P = 0.0016$) than the other 30 patients.

Liver stiffness and fibrosis stage

The liver stiffness measurements are shown according to the stage of fibrosis in Figure 2. Of the 50 enrolled patients with chronic HBV, 20 (40%) were classified as F1, 10 (20%) as F2, 5 (10%) as F3, and 3 (6%) as F4 on liver biopsies; cirrhosis was clinically diagnosed in 12 (24%) patients. When clinical cirrhosis was combined with histological F4, median liver stiffness (interquartile range) was 7.0 kPa (5.6–9.4), 9.8 kPa (5.6–14.7), 9.8 kPa (7.6–12.9), and 17.3 kPa (8.2–27.6) in fibrosis stages F1 to F4, respectively. Liver stiffness significantly correlated with the stage of fibrosis ($r = 0.46$;

Table 1 Baseline characteristics of patients

	All patients ($n = 50$)	Patients who started entecavir ($n = 20$)
Age (years)†	50 ± 13	50 ± 14
Sex (male/female)‡	28/22	14/6
Body mass index (kg/m^2)†	22.4 ± 2.7	22.1 ± 2.8
ALT (IU/L)§	75 (40–125)	111 (67–186)
Platelet count (×10^9/L)†	158 ± 63	152 ± 57
HBeAg (+/−)‡	27/23	8/12
HBV DNA ($\log_{10}$ copies/mL)†	5.9 ± 2.1	7.0 ± 1.1
HBV genotype (A/B/C/D)‡	1/4/39/0	1/2/17/0
Grade of necroinflammation‡ (A1/A2/A3)	19/17/2	10/6/1
Stage of fibrosis‡ (F1/F2/F3/F4¶)	20/10/5/15	6/8/4/2

†Mean ± SD; ‡Numbers of patients; §Median (interquartile range). ¶F4 includes cirrhosis clinically diagnosed on the basis of specific signs.
ALT, alanine aminotransferase; HBeAg, hepatitis B e antigen; HBV, hepatitis B virus.

$P = 0.0014$). At the F1 to F4 stages of fibrosis, there was no significant correlation of liver stiffness with serum ALT levels ($r = 0.40$, 0.097, 0.60, and 0.11; $P = 0.083$, 0.77, 0.23, and 0.69, respectively) or with histological necroinflammatory activity ($r = 0.10$, 0.12, 0.71, and 0.50; $P = 0.67$, 0.73, 0.16, and 0.48, respectively).

Liver stiffness during entecavir treatment

Among the 20 patients who started entecavir, 6 (30%) were histologically classified as F1, 8 (40%) as F2, 4 (20%) as F3, and 1 (5%) as F4; cirrhosis was clinically diagnosed in 1 (5%) patient. Serum HBV DNA levels decreased to below the lower detection limit of the PCR assay in 8 (40%) patients at 3 months, 16 (80%) patients at 6 months, and 19 (95%) patients at 12 months. Serum ALT levels decreased to within the reference range in 5 (25%) patients at 3 months, 12 (60%) patients at 6 months, and 14 (70%) patients at 12 months. The changes in liver stiffness during the first 12 months of entecavir treatment are shown in Figure 3. Median liver stiffness (interquartile range) significantly decreased from 11.2 (7.0–15.2) kPa to 7.8 (5.1–11.9) kPa ($P = 0.0090$) during the 12 months. The rate of decrease in liver stiffness did not correlate with the rate of decrease in serum ALT levels ($r = 0.38$; $P = 0.88$).

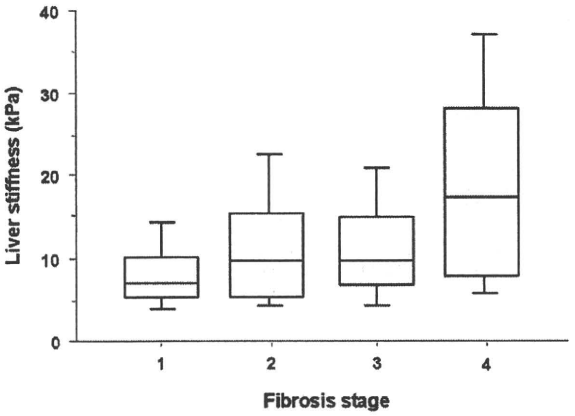

Figure 2 Box plots of liver stiffness measurements according to the stage of fibrosis in all patients with chronic hepatitis B virus. The length of the box represents the interquartile range, within which 50% of the values are located. The lines in the boxes represent the median values. The error bars represent the minimum and maximum values (range). The stage of fibrosis significantly correlated with liver stiffness ($r = 0.46$; $P = 0.0014$).

Serum fibrosis markers during entecavir treatment

The changes in serum fibrosis marker levels during the first 12 months of therapy in the 20 patients treated with entecavir are shown in Figure 4. Median PIIINP levels significantly decreased from 0.9 (0.6–1.3) U/mL to 0.6 (0.5–0.7) U/mL ($P = 0.0010$). Median levels of type IV collagen 7S domain significantly decreased from 5.0 ng/mL (4.4–6.7) to 3.9 ng/mL (3.2–4.4; $P = 0.015$). The rate of decrease in liver stiffness significantly correlated with the rate of decrease in serum PIIINP levels ($r = 0.46$; $P = 0.040$), but not with the rate of decrease in type IV collagen 7S domain levels ($r = 0.27$; $P = 0.26$).

Case presentations

Figures 5 and 6 show the results of paired liver biopsies in two patients, performed at baseline and after

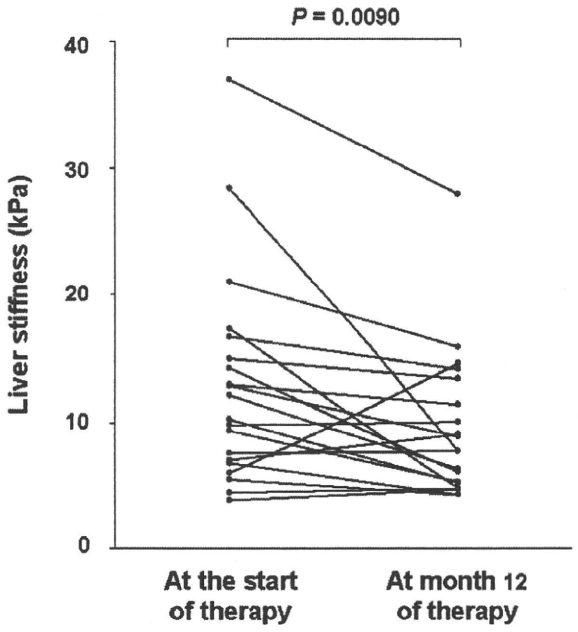

Figure 3 Changes in liver stiffness during the first 12 months of therapy in the 20 patients treated with entecavir. Median liver stiffness (interquartile range) significantly decreased from 11.2 kPa (7.0–15.2) to 7.8 kPa (5.1–11.9; $P = 0.0090$) during the 12 months.

12 months of entecavir treatment. One patient (case 1) was a 41-year-old man in whom the percentage decrease in liver stiffness was highest during the 12 months of treatment (28.4 kPa at baseline, 7.8 kPa at 12 months). The pretreatment HBV DNA level was 7.4 $\log_{10}$ copies/mL and became undetectable on PCR by month 6. The ALT activity was 215 IU/L and fell to the normal range by month 6. The histological grade and stage improved from A2/F4 to A1/F3. The proportion of fibrosis area on morphometric analysis decreased from 12.3% to 8.3% in specimens stained with Sirius red (Fig. 5a) and from 7.0% to 3.7% in specimens stained with α-smooth muscle actin (Fig. 5b). Serum markers of liver fibrosis also decreased (PIIINP, 1.4 U/mL to 0.5 U/mL; type IV collagen 7S domain, 7.1 ng/mL to 3.8 ng/mL).

The other patient (case 2) was a 45-year-old man who had the greatest increase in liver stiffness (6.0 kPa at

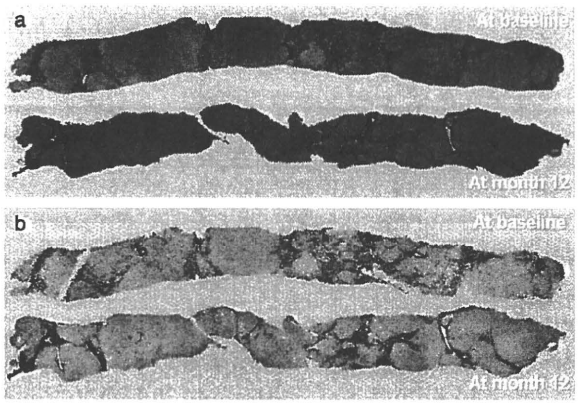

Figure 5 Paired liver biopsies performed in case 1 at baseline and after 12 months of entecavir treatment. The proportion of fibrosis area on morphometry decreased from (a) 12.3% at baseline to 8.3% after 12 months of therapy in specimens stained with Sirius red, and (b) from 7.0% to 3.7% in specimens stained with α-smooth muscle actin.

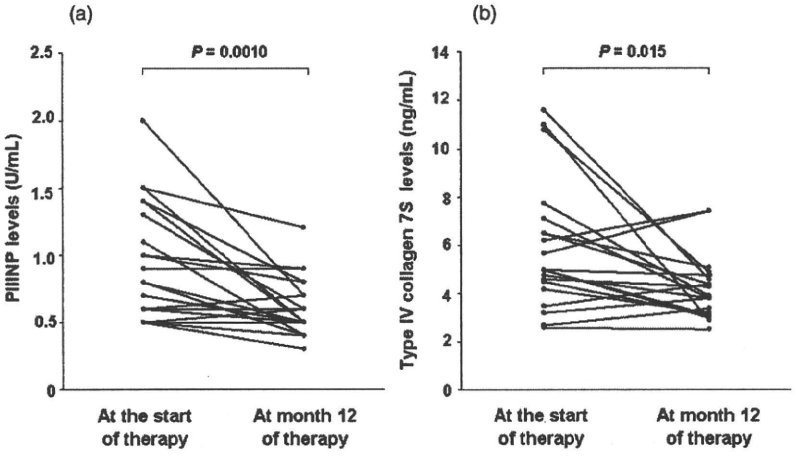

Figure 4 Changes in serum fibrosis marker levels during the first 12 months of therapy in the 20 patients treated with entecavir. There were significant decreases in the levels of (a) peptide of type III procollagen (PIIINP; $P = 0.0010$) and (b) type IV collagen 7S domain in serum ($P = 0.015$).

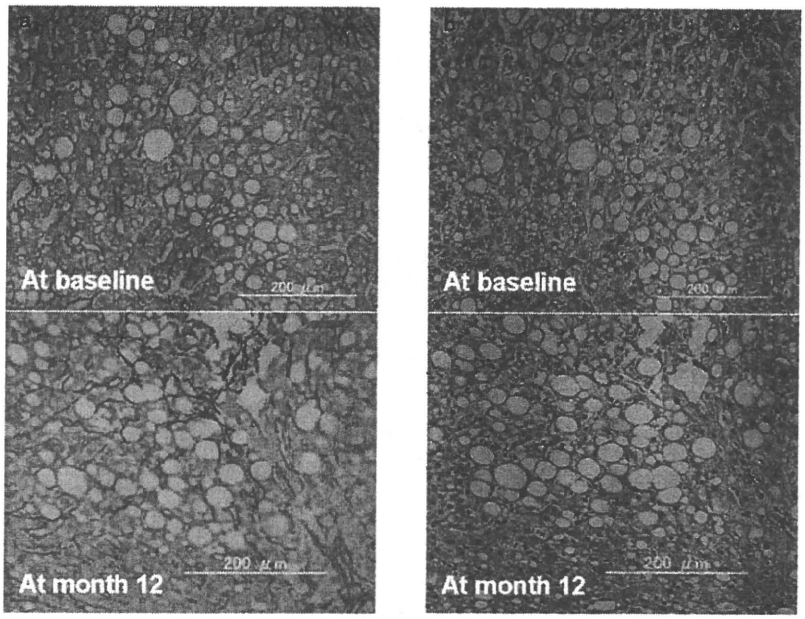

Figure 6 Paired liver biopsies performed in case 2 at baseline and after 12 months of entecavir treatment. The proportion of fibrosis area on morphometry increased from (a) 3.4% to 4.4% on Sirius red staining, and (b) from 0.9% to 1.5% on α-smooth muscle actin staining. At baseline, hepatic steatosis involved less than 5% of the biopsy specimen; the presence of steatosis was noted at the second biopsy involving about 20% of the specimen. The perisinusoidal/pericellular fibrosis was seen around hepatocytes distended by steatosis.

baseline to 14.5 kPa at 12 months). He did not drink alcohol, but body weight increased by 3.0 kg during the 12 months of treatment. Although the HBV DNA level rapidly decreased from 7.6 $\log_{10}$ copies/mL to below the detection limit by month 7, ALT activity did not fall significantly from baseline value (41 IU/L). The results of histological evaluations were unchanged on the paired biopsies performed 12 months apart (A1/F2). The proportion of fibrosis area on morphometric analysis increased from 3.4% to 4.4% on Sirius red staining (Fig. 6a) and from 0.9% to 1.5% on α-smooth muscle actin staining (Fig. 6b). On the second biopsy, the presence of hepatic steatosis was noted, involving about 20% of the biopsy specimen; perisinusoidal/pericellular fibrosis was seen around hepatocytes distended by steatosis. Serum fibrosis markers also did not decrease (PIIINP, 0.9 U/mL to 0.9 U/mL; type IV collagen 7S domain, 4.8 ng/mL to 5.0 ng/mL).

DISCUSSION

OF THE 50 patients studied, 45 were Japanese, two were Chinese, two Korean, and one Philippine. In Japan and other countries in east Asia, genotype C is the most prevalent type of HBV,[18,19] and most patients with chronic HBV acquire the virus perinatally or in early childhood.[20] The rates of virological and biochemical responses to interferon are thus lower than those reported in Europe and the United States. Guidelines proposed by the Japanese Study Group of the Standardization of Treatment of Viral Hepatitis Including Cirrhosis recommend that nucleos(t)ide-naïve patients with chronic HBV who are 35 years or older should receive entecavir as the treatment of choice.[21] In our patients, characterized by a predominance of genotype C, the rate of response to entecavir was similar to the rates obtained in randomized controlled trials conducted worldwide.[4,5]

Liver stiffness as measured by transient elastography significantly correlated with the stage of fibrosis in our patients with chronic HBV (Fig. 2), consistent with the results of previous studies.[12,13] Factors other than fibrosis, including necroinflammatory activity,[22–24] obesity,[25] and extrahepatic cholestasis,[26] can affect the results of liver stiffness measurement. In particular, chronic HBV is associated with more frequent acute exacerbations than chronic hepatitis C. In this study, we did not include patients with acute exacerbation. There was no significant correlation between liver stiffness and serum ALT levels or histological necroinflammatory activity. No patient was obese as defined by a body mass index of >30 kg/m^2.

Liver stiffness measurement is generally less accurate for the diagnosis of liver fibrosis in chronic HBV than in chronic hepatitis C.[27] In previous studies that included both chronic HBV and C,[28,29] median liver stiffness at each stage of fibrosis was lower in chronic HBV than in

chronic hepatitis C. The reported cutoff value for predicting cirrhosis in chronic HBV ranged from 9.0 to 11.0 kPa,[30,31] which is lower than 13.0 kPa, the optimal cutoff value based on a meta-analysis of 17 studies of various chronic liver diseases (mostly chronic hepatitis C).[13] In the present study, liver stiffness was lower than 13.0 kPa in 5 (33%) of the 15 patients with cirrhosis (data not shown). In addition, it was difficult to predict advanced fibrosis (≥F3), since median liver stiffness was similar in F2 and F3 (9.8 kPa). One possible explanation for difference in diagnostic accuracy is that the amount of fibrosis in the cirrhotic liver is lower in chronic HBV than in chronic hepatitis C because macronodular cirrhosis, characterized by large nodules delimited by thin septa, is more common in patients chronically infected with HBV.

Median liver stiffness as measured by transient elastography significantly decreased during the 12 months of entecavir treatment (Fig. 3). Our results may reflect an improvement in liver fibrosis by treatment with entecavir, similar to that demonstrated in a *post hoc* descriptive analysis of randomized controlled trials.[6] To exclude the possibility that the decrease in liver stiffness was caused by regression of necroinflammatory activity, we also measured the levels of serum markers of liver fibrosis. In general, liver fibrosis markers can be divided into two groups, either direct or indirect. Direct markers of fibrosis reflect serum extracellular matrix turnover. For example, PIIINP, a product formed by cleavage of procollagen III, is released into the serum during matrix deposition.[32] Type IV collagen 7S domain is located in basement membranes and released during interstitial filament degradation, thereby reflecting matrix degradation.[33] In this study, both markers significantly decreased during the 12 months of entecavir treatment (Fig. 4).

Indirect markers of liver fibrosis reflect alterations in hepatic function, but do not directly reflect hepatic extracellular matrix metabolism. Indirect markers include platelet count, the results of coagulation studies, hepatic aminotransferases, and combined indices/scores derived from these variables. Combined indices/scores such as aspartate aminotransferase/ALT ratio,[34] aspartate aminotransferase-to-platelet ratio index,[35] cirrhosis discriminant score,[36] and Lok index,[37] are not suitable for on-treatment assessment of liver fibrosis in chronic HBV, because these indices/scores include hepatic aminotransferases, which rapidly decrease after the start of antiviral treatment.

Many studies have shown significant correlations between the results of morphometric image analysis and those of semiquantitative histological staging,[38,39] although potential limitations of morphometry include the sampling error. On liver biopsy, only 1/50 000 of the organ (and 1/100 of the region of interest for liver stiffness measurement) is analyzed. In addition, to accurately measure liver fibrosis, it is necessary to carefully exclude necroinflammation in fibrous areas, requiring significant time and labor, even for a trained hepatopathologist. We did a morphometric analysis in two patients with paired liver biopsy specimens stained with Sirius red for collagen or with α-smooth muscle actin for activated hepatic stellate cells. One patient (case 1) showed regression of both histological stage and extent of fibrosis on morphometry. The results of liver stiffness measurement and serum fibrosis markers also improved. More interestingly, in the other patient (case 2), both the extent of fibrosis as estimated by morphometry and liver stiffness increased, despite a virological response to entecavir. We speculate that pericellular fibrosis caused by steatohepatitis was the main cause of increase in liver stiffness in this patient. In the previous study,[40] liver stiffness correlated more strongly with pericellular fibrosis than with periportal or perivenular fibrosis. The histological stage of fibrosis was unchanged, probably because it reflects liver architectural abnormalities, not directly the amount of fibrosis. If liver stiffness increases during antivairal treatment for chronic HBV, liver biopsy should be considered to exclude other potential causes of chronic liver disease.

The major limitation of this study is the short duration of observation during entecavir treatment. In the 5 patients treated with entecavir for more than 24 months, median liver stiffness decreased slightly, but not significantly from 7.8 kPa to 7.0 kPa during the second 12 months of entecavir treatment (data not shown). The decrease in liver stiffness during the second 12 months of treatment might be attributed solely to an improvement in liver fibrosis, not an improvement in necroinflammation. Another limitation of this study is the small number of patients. The rate of decrease in liver stiffness significantly correlated with rate of decrease in the serum level of PIIINP, but not with that of type IV collagen 7S domain, possibly because of an insufficient number of patients. Larger studies are required to confirm the usefulness of transient elastography as a tool for on-treatment monitoring of the regression of liver fibrosis.

In conclusion, transient elastography is a rapid, noninvasive, objective, and promising technique for the assessment of fibrosis by measuring liver stiffness in

patients with chronic HBV, as well as those with chronic hepatitis C virus. Liver stiffness measurement might be useful for monitoring regression of liver fibrosis during entecavir treatment for chronic HBV.

ACKNOWLEDGMENTS

THE AUTHORS ARE grateful to Ms Sanae Deguchi and Ms Rie Yasuda for technical assistance.

REFERENCES

1 Dienstag JL. Hepatitis B virus infection. *N Engl J Med* 2008; **359**: 1486–500.
2 Lok AS, McMahon BJ. Chronic hepatitis B: update 2009. *Hepatology* 2009; **50**: 661–2.
3 European Association for The Study of the Liver. EASL Clinical Practice Guidelines: management of chronic hepatitis B. *J Hepatol* 2009; **50**: 227–42.
4 Chang TT, Gish RG, de Man R *et al.* A comparison of entecavir and lamivudine for HBeAg-positive chronic hepatitis B. *N Engl J Med* 2006; **354**: 1001–10.
5 Lai CL, Shouval D, Lok AS *et al.* Entecavir versus lamivudine for patients with HBeAg-negative chronic hepatitis B. *N Engl J Med* 2006; **354**: 1011–20.
6 Schiff E, Simsek H, Lee WM *et al.* Efficacy and safety of entecavir in patients with chronic hepatitis B and advanced hepatic fibrosis or cirrhosis. *Am J Gastroenterol* 2008; **103**: 2776–83.
7 Perrault J, McGill DB, Ott BJ, Taylor WF. Liver biopsy: complications in 1000 inpatients and outpatients. *Gastroenterology* 1978; **74**: 103–6.
8 Janes CH, Lindor KD. Outcome of patients hospitalized for complications after outpatient liver biopsy. *Ann Intern Med* 1993; **118**: 96–8.
9 Afdhal NH, Nunes D. Evaluation of liver fibrosis: a concise review. *Am J Gastroenterol* 2004; **99**: 1160–74.
10 Pinzani M, Vizzutti F, Arena U, Marra F. Technology Insight: noninvasive assessment of liver fibrosis by biochemical scores and elastography. *Nat Clin Pract Gastroenterol Hepatol* 2008; **5**: 95–106.
11 Yoshioka K, Kawabe N, Hashimoto S. Transient elastography: applications and limitations. *Hepatol Res* 2008; **38**: 1063–8.
12 Castera L, Forns X, Alberti A. Non-invasive evaluation of liver fibrosis using transient elastography. *J Hepatol* 2008; **48**: 835–47.
13 Friedrich-Rust M, Ong MF, Martens S *et al.* Performance of transient elastography for the staging of liver fibrosis: a meta-analysis. *Gastroenterology* 2008; **134**: 960–74.
14 Bedossa P, Poynard T. An algorithm for the grading of activity in chronic hepatitis C. The METAVIR Cooperative Study Group. *Hepatology* 1996; **24**: 289–93.
15 Usuda S, Okamoto H, Iwanari H *et al.* Serological detection of hepatitis B virus genotypes by ELISA with monoclonal antibodies to type-specific epitopes in the preS2-region product. *J Virol Methods* 1999; **80**: 97–112.
16 Ide T, Kumashiro R, Hino T *et al.* Transcription-mediated amplification is more useful in the follow-up of patients with chronic hepatitis B treated with lamivudine. *Hepatol Res* 2001; **21**: 76–84.
17 Gerken G, Gomes J, Lampertico P *et al.* Clinical evaluation and applications of the Amplicor HBV Monitor test, a quantitative HBV DNA PCR assay. *J Virol Methods* 1998; **74**: 155–65.
18 Orito E, Ichida T, Sakugawa H *et al.* Geographic distribution of hepatitis B virus (HBV) genotype in patients with chronic HBV infection in Japan. *Hepatology* 2001; **34**: 590–4.
19 Enomoto M, Tamori A, Nishiguchi S. Hepatitis B virus genotypes and response to antiviral therapy. *Clin Lab* 2006; **52**: 43–7.
20 Liaw YF, Leung N, Kao JH *et al.* Asian-Pacific consensus statement on the management of chronic hepatitis B: a 2008 update. *Hepatol Int* 2008; **2**: 263–83.
21 Kumada H, Okanoue T, Onji M *et al.* Guidelines for the treatment of chronic hepatitis and cirrhosis due to hepatitis B virus infection for the fiscal year 2008 in Japan. *Hepatol Res* 2010; **40**: 1–7.
22 Arena U, Vizzutti F, Corti G *et al.* Acute viral hepatitis increases liver stiffness values measured by transient elastography. *Hepatology* 2008; **47**: 380–4.
23 Sagir A, Erhardt A, Schmitt M, Häussinger D. Transient elastography is unreliable for detection of cirrhosis in patients with acute liver damage. *Hepatology* 2008; **47**: 592–5.
24 Wong GL, Wong VW, Choi PC *et al.* Increased liver stiffness measurement by transient elastography in severe acute exacerbation of chronic hepatitis B. *J Gastroenterol Hepatol* 2009; **24**: 1002–7.
25 Fraquelli M, Rigamonti C, Casazza G *et al.* Reproducibility of transient elastography in the evaluation of liver fibrosis in patients with chronic liver disease. *Gut* 2007; **56**: 968–73.
26 Millonig G, Reimann FM, Friedrich S *et al.* Extrahepatic cholestasis increases liver stiffness (FibroScan) irrespective of fibrosis. *Hepatology* 2008; **48**: 1718–23.
27 Ganne-Carrié N, Ziol M, de Ledinghen V *et al.* Accuracy of liver stiffness measurement for the diagnosis of cirrhosis in patients with chronic liver diseases. *Hepatology* 2006; **44**: 1511–7.
28 Coco B, Oliveri F, Maina AM *et al.* Transient elastography: a new surrogate marker of liver fibrosis influenced by major changes of transaminases. *J Viral Hepat* 2007; **14**: 360–9.
29 Ogawa E, Furusyo N, Toyoda K *et al.* Transient elastography for patients with chronic hepatitis B and C virus infec-

tion: Non-invasive, quantitative assessment of liver fibrosis. *Hepatol Res* 2007; **37**: 1002–10.
30 Chan HL, Wong GL, Choi PC *et al.* Alanine aminotransferase-based algorithms of liver stiffness measurement by transient elastography (Fibroscan) for liver fibrosis in chronic hepatitis B. *J Viral Hepat* 2009; **16**: 36–44.
31 Marcellin P, Ziol M, Bedossa P *et al.* Non-invasive assessment of liver fibrosis by stiffness measurement in patients with chronic hepatitis B. *Liver Int* 2009; **29**: 242–7.
32 McCullough AJ, Stassen WN, Wiesner RH, Czaja AJ. Serum type III procollagen peptide concentrations in severe chronic active hepatitis: relationship to cirrhosis and disease activity. *Hepatology* 1987; **7**: 49–54.
33 Murawaki Y, Ikuta Y, Koda M, Yamada S, Kawasaki H. Comparison of serum 7S fragment of type IV collagen and serum central triple-helix of type IV collagen for assessment of liver fibrosis in patients with chronic viral liver disease. *J Hepatol* 1996; **24**: 148–54.
34 Williams AL, Hoofnagle JH. Ratio of serum aspartate to alanine aminotransferase in chronic hepatitis. Relationship to cirrhosis. *Gastroenterology* 1988; **95**: 734–9.
35 Wai CT, Greenson JK, Fontana RJ *et al.* A simple noninvasive index can predict both significant fibrosis and cirrhosis in patients with chronic hepatitis C. *Hepatology* 2003; **38**: 518–26.
36 Bonacini M, Hadi G, Govindarajan S, Lindsay KL. Utility of a discriminant score for diagnosing advanced fibrosis or cirrhosis in patients with chronic hepatitis C virus infection. *Am J Gastroenterol* 1997; **92**: 1302–4.
37 Lok AS, Ghany MG, Goodman ZD *et al.* Predicting cirrhosis in patients with hepatitis C based on standard laboratory tests: results of the HALT-C cohort. *Hepatology* 2005; **42**: 282–92.
38 Goodman ZD, Becker RL, Pockros PJ *et al.* Progression of fibrosis in advanced chronic hepatitis C: evaluation by morphometric image analysis. *Hepatology* 2007; **45**: 886–94.
39 Nitta Y, Kawabe N, Hashimoto S *et al.* Liver stiffness measured by transient elastography correlates with fibrosis area in liver biopsy in patients with chronic hepatitis C. *Hepatol Res* 2009; **39**: 675–84.
40 Wong GL, Wong VW, Choi PC *et al.* Assessment of fibrosis by transient elastography compared with liver biopsy and morphometry in chronic liver diseases. *Clin Gastroenterol Hepatol* 2008; **6**: 1027–35.

See related Commentary on page 10

The American Journal of Pathology, Vol. 177, No. 1, July 2010

DOI: 10.2353/ajpath.2010.090895

Gastrointestinal, Hepatobiliary and Pancreatic Pathology

A Human-Type Nonalcoholic Steatohepatitis Model with Advanced Fibrosis in Rabbits

Tomohiro Ogawa,* Hideki Fujii,* Katsutoshi Yoshizato,*† and Norifumi Kawada*

From the Department of Hepatology, Graduate School of Medicine, Osaka City University, Osaka, and PhoenixBio Co. Ltd.,† Hiroshima, Japan*

Nonalcoholic steatohepatitis (NASH) progresses to liver fibrosis and cirrhosis, which can lead to life-threatening liver failure and the development of hepatocellular carcinoma. The aim of the present study was to create a rabbit model of NASH with advanced fibrosis (almost cirrhosis) by feeding the animals a diet supplemented with 0.75% cholesterol and 12% corn oil. After 9 months of feeding with this diet, the rabbits showed high total cholesterol levels in serum and liver tissues in the absence of insulin resistance. The livers became whitish and nodular. In addition, the number of rabbit macrophage antigen-positive cells and the expression of mRNAs for inflammatory cytokines showed a significant increase. Moreover, fibrotic septa composed of collagens and α-smooth muscle actin-positive cells were found between the central and portal veins, indicating alteration of the parenchymal architecture. There was also a marked increase of mRNAs for transforming growth factor-β1 and collagen 1A1. Comprehensive analysis of protein and gene expression revealed an imbalance of the antioxidant system and methionine metabolism. We also found that ezetimibe attenuated steatohepatitis in this model. In conclusion, the present rabbit model of NASH features advanced fibrosis that is close to cirrhosis and may be useful for analyzing the molecular mechanisms of human NASH. Ezetimibe blunted the development of NASH in this model, suggesting its potential clinical usefulness for human steatohepatitis. ***(Am J Pathol 2010, 177:153–165; DOI: 10.2353/ajpath.2010.090895)***

A high-fat diet is one of the risk factors for metabolic syndrome, which is characterized by obesity, hyperlipidemia, hyperglycemia, and hypertension, and is frequently accompanied by life-threatening arteriosclerosis.[1] A high-calorie, high-fat diet is also considered to cause nonalcoholic fatty liver disease (NAFLD), which covers a spectrum of disorders from simple steatosis to nonalcoholic steatohepatitis (NASH) and cirrhosis.[2–5] Recent clinical studies have shown that NAFLD is one of the common liver diseases that leads to cirrhosis and hepatocellular carcinoma[2] in a manner similar to the clinical course of chronic viral hepatitis and alcohol abuse.[6] However, the molecular mechanisms underlying the progression of NAFLD to an advanced stage with active inflammation and fibrosis are not fully understood. We recently reported a rabbit model of steatohepatitis that was generated by feeding the rabbit a high-fat and -cholesterol diet (HFD) supplemented with 20% corn oil and 1.25% (w/w) cholesterol for 8 weeks.[7] The rabbit showed insulin resistance, accumulation of lipids in hepatocytes, activation of Kupffer cells (liver macrophages), mild fibrosis, and enhanced oxidative stress. Thus, we concluded that this model was useful for analyzing the molecular mechanisms involved in the pathogenesis of human NASH. However, rabbits fed a HFD have a short lifespan attributable to heart failure accompanied by severe arteriosclerosis.[8] This makes it difficult to study whether advanced fibrosis or even cirrhosis can be caused solely by HFD feeding. We therefore tried to improve the model and produce NASH with advanced fibrosis, which is more similar to the disease observed in humans that gradually develops after several decades. In the present study, this was accomplished by reducing the concentrations of cholesterol and corn oil in the diet and by prolonging the feeding period from 2 to 9 months.

Supported by the Japan Society for the Promotion of Science (grant-in-aid for scientific research 18659214, 2007, to N.K.) and by a Thrust Area research grant from Osaka City University (2008) (N.K.).

Accepted for publication March 22, 2010.

Portions of this study were presented in abstract form at the 44th Annual Meeting of the European Association for the Study of the Liver, Copenhagen, 2009.

CME Disclosure: None of the authors disclosed any relevant financial relationships.

Supplemental material for this article can be found on *http://ajp.amjpathol.org*.

Address reprint requests to Norifumi Kawada, M.D., Ph.D., Department of Hepatology, Graduate School of Medicine, Osaka City University, 1-4-3, Asahimachi, Abeno, Osaka 545-8585, Japan. E-mail: kawadanori@med.osaka-cu.ac.jp.

NAFLD/NASH is assumed to be most effectively improved by weight control and by restricting lipid and calorie intake, thereby leading to normalized lipid metabolism.[9,10] Nevertheless, drug therapy would be a useful and an easy option because the modern lifestyle habits such as poor diet and lack of regular exercise are difficult to change. Ezetimibe is a relatively new and promising drug candidate for NAFLD/NASH therapy. Ezetimibe selectively inhibits cholesterol absorption via Niemann-Pick C1-like 1 (NPC1L1) protein in the brush border of the small intestine in humans, rodents, rabbits, and other species.[11–15] It decreases the serum levels of low-density lipoprotein cholesterol and triglycerides (TGs) in humans[16] and reduces plaque formation and improves lipids in a rabbit model of atherosclerosis.[17] Recent reports have indicated that ezetimibe improves liver steatosis and insulin resistance in Zucker obese fatty rats[18] and rats fed a methionine- and choline-deficient diet.[19] Thus, ezetimibe is a potential new therapeutic agent for human NASH.[20] In the present study, we also assessed the effect of ezetimibe on the development of NASH in our rabbit model.

Materials and Methods

Materials

Mouse monoclonal antibodies against α-smooth muscle actin (αSMA), rabbit macrophage (clone RAM-11), and 4-hydroxy-2-nonenal (4-HNE) were obtained from Sigma Chemical Co. (St. Louis, MO), Thermo Fisher Scientific (Fremont, CA), and Nikken Seil Co., Ltd. (Shizuoka, Japan), respectively. Enhanced chemiluminescence detection reagent was obtained from Amersham Pharmacia Biotech (Little Chalfont, Buckinghamshire, UK), and Immobilon-P membranes were from Millipore Corp. (Bedford, MA). All other reagents were purchased from Sigma Chemical Co. or Wako Pure Chemical Co. (Osaka, Japan).

Animals and Experimental Protocol

Pathogen-free male Japanese White rabbits, about 1-year-old and weighing 3.0 to 3.5 kg, were obtained from SLC (Shizuoka, Japan). As shown in Figure 1, we performed the following two experiments: i) rabbits were housed at a constant temperature and were given either 100 g/day of a standard diet (SD) (n = 5, CR3 obtained from CLEA Japan Inc., Tokyo, Japan) or version II of an improved high-fat and -cholesterol diet (HFD II) (n = 5), which consisted of SD supplemented with 12% corn oil and 0.75% (w/w) cholesterol for 9 months; and ii) rabbits were given version I (100 g/day) of a previously reported HFD (HFD I), which consisted of SD supplemented with 20% corn oil and 1.25% (w/w) cholesterol for 2 months.[7] The treated group additionally received 0.6 mg/kg/day of ezetimibe mixed in the diet. Ezetimibe was kindly provided by Bayer AG (Leverkusen, Germany). The contents of the SD and HFD I and II are shown in Supplemental Table S1 (see *http://ajp.amjpathol.org*).

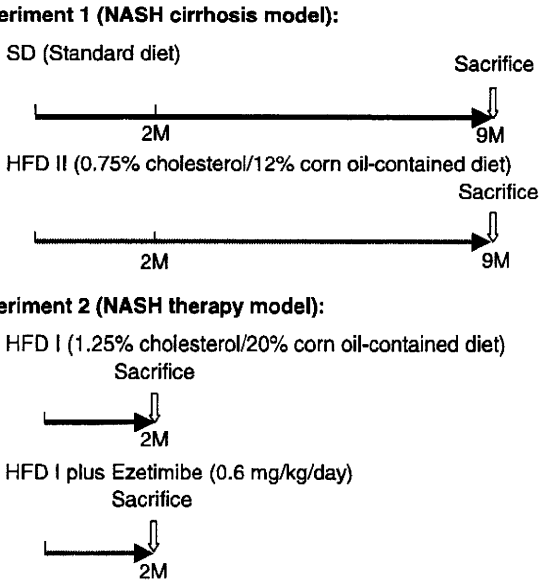

Figure 1. Experimental schedule of the present study. Experiment 1: NASH cirrhosis was induced in rabbits by feeding HFD II for nine months. Experiment 2: during NASH therapy, rabbits were administrated ezetimibe (0.6 mg/kg/day) supplemented with HFD I for two months. In the NASH therapy model, a previously reported HFD I was used to evaluate the effect of medicine during a short period.

The rabbits were fasted 24 hours before sacrifice. Then they were anesthetized and laparotomized for blood and liver sampling. The portal vein was cannulated using an 18-gauge Teflon catheter. The liver of each animal was perfused with 100 ml of PBS to remove the blood. After harvest, the liver was cut into small pieces and fixed in 4% paraformaldehyde. Each sample was either frozen or embedded in paraffin. The experiments were conducted humanely in accordance with the recommendations of the Guide for the Care and Use of Laboratory Animals of Osaka City University School of Medicine.

Histochemical and Immunohistochemical Studies

Paraformaldehyde-fixed specimens were sectioned into 5-μm-thick sections and stained with H&E and 0.1% (w/v) Sirius red (Direct Red 80, Aldrich, Milwaukee, WI). Frozen sections (5-μm-thick) were stained with Oil red O (Wako Pure Chemical Co.). The areas stained by Sirius red and Oil red O were measured to assess the areas of connective tissue and lipid deposition, respectively, using an image analyzer (Lumina Vision, Mitani Corporation, Tokyo, Japan).

Immunohistochemical analysis was performed as described elsewhere.[7] In brief, sections were deparaffinized, washed, and preincubated in 5% bovine serum albumin blocking solution, followed by overnight incubation at 4°C with antibodies against either αSMA at a dilution of 1:100, rabbit macrophage (RAM-11)[21] at a dilution of 1:100, or 4-HNE at a concentration of 5 μg/ml.[22] The sections were incubated with biotinylated sec-

ondary antibodies and reacted with horseradish peroxidase-conjugated streptavidin (Nichirei Biosciences Inc., Tokyo, Japan) and then treated with diaminobenzidine (DAKO, Glostrup, Denmark) for color development.

Laboratory Tests

Serum levels of aspartate aminotransferase (AST), alanine aminotransferase (ALT), total cholesterol (T-Cho), TG, free fatty acid (FFA), and fasting glucose were measured at the Special Reference Laboratories (Osaka, Japan). Fractionation of serum cholesterol was performed by high-performance liquid chromatography at Skylight Biotech (Akita, Japan). The serum and urine levels of oxidative stress markers and antioxidants were measured at Nikken Seil Co., Ltd. Fasting serum insulin levels were measured using a rat insulin enzyme-linked immunosorbent assay kit and a rabbit insulin standard solution (Shibayagi Co. Ltd., Gunma, Japan). Homeostasis model assessment of insulin resistance (HOMA-IR) was calculated using the formula HOMA-IR = [fasting insulin (ng/ml) × 23.1] × fasting glucose (mg/dl)/405. Serum bile acid was measured using a Total Bile Acids Test Wako (Wako Pure Chemical Co.) according to the manufacturer's instructions.

Assay of Hepatic Total Cholesterol, Triglyceride, and Free Fatty Acid Levels

Liver tissue (50 to 100 mg) was homogenized in 0.75 ml of methanol and chloroform (2:1), and lipids were extracted from the chloroform fraction. Then, the hepatic tissue levels of T-Cho and TG were determined using a Cholesterol E-Test Wako and Triglyceride E-Test Wako (Wako Pure Chemical Co.) according to the manufacturer's instructions. The data were expressed as the amount of T-Cho (mg) or TG (mg)/liver wet weight (g).

For the hepatic FFA assay, liver tissue (10 mg) was homogenized in 0.2 ml of chloroform and 1% Triton X-100. Fatty acids were extracted in the chloroform fraction and air-dried to remove the chloroform. Then, the hepatic tissue FFA levels were determined using a Free Fatty Acid Quantification Kit (BioVision, Mountain View, CA) according to the manufacturer's instructions. The data were expressed as the amount of FFA (nmol)/liver wet weight (mg).

Quantitative Real-Time PCR

Total RNA was extracted from the liver using Isogen (Nippon Gene Co. Ltd., Tokyo, Japan). cDNAs were synthesized with 1 μg of total RNA, ReverTra Ace (Toyobo, Osaka, Japan), and oligo(dT)$_{12\text{-}18}$ primers according to the manufacturer's instructions.[23] Gene expression was measured by real-time PCR on an Applied Biosystems Prism 7500 system (Applied Biosystems, Foster City, CA) using cDNA, real-time PCR Master Mix Reagents (Toyobo), a set of gene-specific oligonucleotide primers, and the TaqMan probes listed in Table 1.

Immunoblotting

Protein samples (10 μg) were subjected to SDS-polyacrylamide gel electrophoresis (PAGE) and then transferred to Immobilon-P membranes. After blocking, the membranes were treated with the primary antibodies and then with horseradish peroxidase-conjugated secondary antibodies. Immunoreactive bands were visualized using the enhanced chemiluminescence system and documented with LAS 1000 (Fuji Photo Film, Kanagawa, Japan). The density of each band was analyzed using a GS-700 densitometer (Bio-Rad Laboratories, Hercules, CA).[23]

Assay of Hepatic 8-Hydroxy-2′-Deoxyguanosine Levels

Liver tissue (100 to 200 mg) was homogenized in lysis buffer, and hepatic DNA was extracted using the DNA Extractor TIS kit (Wako Pure Chemical Co.). After the DNA was hydrolyzed, 8-hydroxy-2′-deoxyguanosine levels in the liver were measured using a highly sensitive 8-hydroxy-2′-deoxyguanosine enzyme-linked immunosorbent assay kit (Nikken Seil Co. Ltd.) according to the manufacturer's instructions.

Proteome Analysis

Two-dimensional SDS-PAGE was performed by Towa Environment Science (Osaka, Japan).[24] Proteins (100 μg) extracted from rabbit livers were applied to Immobiline DryStrips (pH 3 to 10). After isoelectric focusing, the proteins were separated by SDS-PAGE on 9 to 18 acrylamide gradient gels, visualized by SYPRO Ruby staining, scanned, and analyzed as described previously.[25] Protein spots of interest were excised from the gels, digested in trypsin solution, dialyzed, and then analyzed by electrospray ionization mass spectrometry. The proteins were identified from the obtained amino acid sequences using databases such as protein BLAST or FASTA.

Microarray Analysis

Total RNA was extracted from liver tissues with Isogen. Rabbit microarray chips were designed on the eArray system (Agilent Technologies, Palo Alto, CA) and were provided by Takara Bio Inc. (Shiga, Japan). The gene expression profile of HFD II-fed rabbits was compared with that of SD-fed rabbits. Genes showing differences in expression with an increase of more than fivefold or a decrease to <0.5-fold were recognized as up- or down-regulated genes, respectively, and were targeted for further analysis. The data are partially shown in Supplemental Table S2 (see *http://ajp.amjpathol.org*).

Statistical Analysis

Bar graphs present data as means ± SD of at least three independent experiments. Statistical analysis was per-

Table 1. List of Primer Sequences

Gene	Sequence	Accession no.
PPARγ		
Forward	5′-CCTGGCTTTGTGAGCCTTGAC-3′	AY166780
Reverse	5′-GAGGCCAGCATGGTGTAGATGA-3′	
aP2		
Forward	5′-CAGATGACAGGAAAGGCAAGAGT-3′	AF136241
Reverse	5′-CCTCCCGTTTTCTCTTTATGGT-3′	
LXRα		
Forward	5′-GGAGACGTCTCGCAGGTACA-3′	
Reverse	5′-CCCTGCTTTGGCAAAGTCCT-3′	
SREBP1		
Forward	5′-GACACAGGAGCCACAATGAAGAC-3′	AF278696
Reverse	5′-GCAGTTTGTCTGTGTCCACAACC-3′	
SREBP2		
Forward	5′-GGCGGACAAGACACAATATCA-3′	AF278693
Reverse	5′-GTCCCCATGACCAAGTCTTTCA-3′	
HMGCR		
Forward	5′-TGCTGTGAGAACGTGATTGGG-3′	
Reverse	5′-CTTTCCATCCAAGCAGAGAGGT-3′	
LDLR		
Forward	5′-ACAACCCGGTCTACCAGAAG-3′	M11501
Reverse	5′-ATCTGTCTCGAGGGGTAGGT-3′	
CYP7A1		
Forward	5′-CGATGCCTTGATTTCCCTCACAG-3′	NM_001170929
Reverse	5′-TTGGTTCAGGACGTCTCAAGGTAAG-3′	
G6Pase		
Forward	5′-GCAGGTGTGTACTACGTGATGGT-3′	EU520488
Reverse	5′-GTCAAGCACCGAAATCTGTAGGTC-3′	
PEPCK		
Forward	5′-CACATCCCAACTCTCGCTTCTG-3′	EF616471
Reverse	5′-TCCAAAGATGATGGCATCAATGGG-3′	
TNFα		
Forward	5′-GTCACCCTCAGATCAGCTTCTC-3′	NM_001082263
Reverse	5′-GTTCGCACGCTGGCTCAG-3′	
Probe	5′-CCTGAGTGACAAGCCTCTAGCCCACG-3′	
IL-1β		
Forward	5′-GCCTGAGAACTTTCTTTTCCTTAATC-3′	M26295
Reverse	5′-GATCGTACTGCATCACACTCAAG-3′	
Probe	5′-AAGAACCCGTCCTCTGCAACACCTGG-3′	
IL-10		
Forward	5′-CCTTGTCGGAGATGATCCAGTT-3′	DQ437508
Reverse	5′-ATGGCTGGACTGTGGTTCTCA-3′	
IL-18		
Forward	5′-GCAACCTGTGTTTGAGGATATGC-3′	NM_001122940
Reverse	5′-CCATGCCTCTAGTATTGCTGTCTT-3′	
TLR2		
Forward	5′-TCTGCACAAGCGGGACTTT-3′	NM_001082781
Reverse	5′-TTCTCGATGCAGTCGATGATGT-3′	
TLR4		
Forward	5′-AGCCATGCGGGTATCATTTT-3′	NM_001082732
Reverse	5′-TCCTGCTGAGAAGGCGATACA-3′	
CD14		
Forward	5′-GCGCTAAACTCCCTCAATCTATC-3′	M90488
Reverse	5′-GCCCTATTCAGCTTGTTGCA-3′	
MD2		
Forward	5′-GAAGGGAGAGACTGTGAATACAACAG-3′	NM_001082787
Reverse	5′-GCTATGGCTTCTACAACACATCTG-3′	
HO-1		
Forward	5′-GGAGAACGCCGAGTTCATGA-3′	AY421756
Reverse	5′-GGCCATCACCAGCTTAAAACC-3′	
Probe	5′-AACTTTCAGAAGGGCCAGGTGACTGCC-3′	
TGFβ1		
Forward	5′-AAGGGCTACCACGCCAACTT-3′	AF000133
Reverse	5′-CGGGTTGTGCTGGTTGTACA-3′	
Probe	5′-TGCCTGGGACCCTGCCCCTAC-3′	
Col1A1		
Forward	5′-ACTGGATTGACCCCAACCA-3′	AY633663
Reverse	5′-TTGCCCCAGTGTCCATGTC-3′	
Probe	5′-CTGCAACCTGGATGCCATCAAGGTC-3′	

(*table continues*)

Table 1. *Continued*

Gene	Sequence	Accession no.
Col3A1		
Forward	5′-CATTGGCCCTGTTTGCTTTT-3′	S83371
Reverse	5′-GTTGGTCACTTGTACTGGTTGACA-3′	
MMP-2		
Forward	5′-TCACTCCTGAGATCTGCACACA-3′	NM_001082209
Reverse	5′-CAAATGAACCGGTCCTTGAAG-3′	
MMP-9		
Forward	5′-GCTCCGGTGGATCAGATGTT-3′	NM_001082203
Reverse	5′-AAGCGGTCCTGGCAGAAGT-3′	
Probe	5′-CACACGACGTCTTCCAGTACCGAGAG-3′	
TIMP-1		
Forward	5′-TGGAAAGTGTCTGCGGGTACT-3′	AY829730
Reverse	5′-TTGTCCAGCGATGAGAAACTC-3′	
TIMP-2		
Forward	5′-TCACGCTCTGTGACTTCATCGT-3′	AF069713
Reverse	5′-TGTGGTTCAGGCTCTTCTTCTG-3′	
Probe	5′-CCCTGGGACTCCCTGAGCAGCA-3′	
GPO		
Forward	5′-AAGGTGCTGCTCATTGAGAATG-3′	NM_001085444
Reverse	5′-TTCTCCTGATGCCCAAACTG-3′	
GST		
Forward	5′-CAAGTGGCTGAGTGAGAAGTTCA-3′	NM_001082252
Reverse	5′-TTGCTCTGCGTGAGCTTGT-3′	
Cu,Zn-SOD		
Forward	5′-TGGTGGTCCACGAGAAAGAAG-3′	L12405
Reverse	5′-CGTTCCCGGTCTTTGTACTCT-3′	
Mn-SOD		
Forward	5′-ATTGCTGCGTGTGCGAATC-3′	L28808
Reverse	5′-TCAATCCCCAGCAGTGGAA-3′	
MAT1A		
Forward	5′-TCCACCTGGACAGAAACGAAGAGGA-3′	
Reverse	5′-TCTCGTCAGTGGCATAGCCGAACA-3′	
GNMT		
Forward	5′-AGGGCTTCAGTGTGACGAGTGT-3′	D13307
Reverse	5′-CGGTTCCAGCGCTCTTTAA-3′	
ST3A1		
Forward	5′-GTGCCCTTCTTGGAATACAACA-3′	NM_001082210
Reverse	5′-TGGAAGGTGGGAAGCAAAG-3′	
GAPDH		
Forward	5′-GCCAAAAGGGTCATCATCTCA-3′	AB231852
Reverse	5′-GTGGTTCACGCCCATCACA-3′	
Probe	5′-CCTCCGCCGATGCCCCCA-3′	

formed with Student's *t*-test, and differences were considered significant at $P < 0.05$.

Results

Hepatic Lipid Deposition in Rabbits Fed High-Fat and -Cholesterol Diet II

Rabbits fed HFD I for 2 months exhibited insulin resistance, hepatic steatosis, inflammation, oxidative stress, and mild fibrosis, thus, showing similarity to human NASH as we reported previously.[7] After the feeding period was increased by reducing the fat and cholesterol content in the diet to 60% of the previous level (HFD II) to prolong rabbit survival, we were able to create a model with advanced hepatic fibrosis that was close to cirrhosis. As shown in Table 2, serum T-Cho and TG levels of rabbits fed HFD II for 9 months increased significantly compared with the levels in rabbits fed SD. The serum cholesterol was mainly very low-density lipoprotein and lipoprotein cholesterol according to the high-performance liquid chromatography analysis. However, serum AST and ALT levels in HFD II-fed rabbits did not change significantly compared with those in SD-fed rabbits. Fasting glucose and insulin values in HFD II-fed rabbits were lower than those in SD-fed rabbits, and HOMA-IR was reduced in HFD-fed rabbits.

The livers of HFD II-fed rabbits were enlarged and whitish with an irregular, partially nodular surface (Figure 2, A and B), showing an appearance that was totally different from the livers of SD-fed rabbits. H&E staining indicated degeneration of hepatocytes predominantly around the central vein area (Figure 2, C and D). At a higher magnification, H&E staining also revealed glassy degeneration of hepatocytes, which was similar to the ballooning of hepatocytes in human NASH, fibrosis, and bile duct proliferation (Figure 2, E and F), as well as atheroma in the aorta (Figure 2, G and H). The hepatocytes were strongly positive for Oil red O staining (Figure 3, A and B), Furthermore, hepatic T-Cho content in-

Table 2. Liver Enzymes and Lipid Profile in Serum

Enzymes/lipids	SD	HFD II	*P* value
AST (IU/L)	43.4 ± 29.9	29.3 ± 22.4	NS
ALT (IU/L)	45.6 ± 36.6	19.7 ± 18.2	NS
Cholesterol (mg/dl)			
Total	19.2 ± 3.8	1161.3 ± 406.5	$P < 0.01$
Chylomicron	0.2 ± 0.2	159.6 ± 161.8	NS
Very low-density lipoprotein	1.7 ± 0.6	733.0 ± 294.6	$P < 0.01$
Low-density lipoprotein	2.7 ± 0.8	241.6 ± 74.5	$P < 0.01$
High-density lipoprotein	14.6 ± 4.2	27.1 ± 12.5	NS
TG (mg/dl)	26.7 ± 11.9	205.5 ± 96.3	$P < 0.01$
FFA (μEq/L)	279.7 ± 150.7	168.4 ± 107.9	NS
Fasting glucose (mg/dl)	132.7 ± 11.0	98.4 ± 47.3	$P < 0.05$
Fasting insulin (ng/ml)	1.1 ± 0.2	0.7 ± 0.2	$P < 0.05$
HOMA-IR	8.4 ± 2.3	5.2 ± 2.6	$P < 0.05$
Bile acid	5.3 ± 1.3	33.7 ± 17.4	$P < 0.05$

NS, not significant.

creased significantly in HFD II-fed rabbits (38.3 ± 21.5 μg/mg liver weight) compared with that in SD-fed rabbits (1.5 ± 0.2 μg/mg liver weight), although the hepatic TG and FFA contents were similar (Figure 3C), indicating that mainly cholesterol had accumulated in the hepatocytes of rabbits fed HFD II. Expression of genes related to fat metabolism, such as peroxisome proliferator-activated receptor-γ (PPARγ) and adipocyte lipid-binding protein (aP2), also known as fatty acid binding protein 4, increased

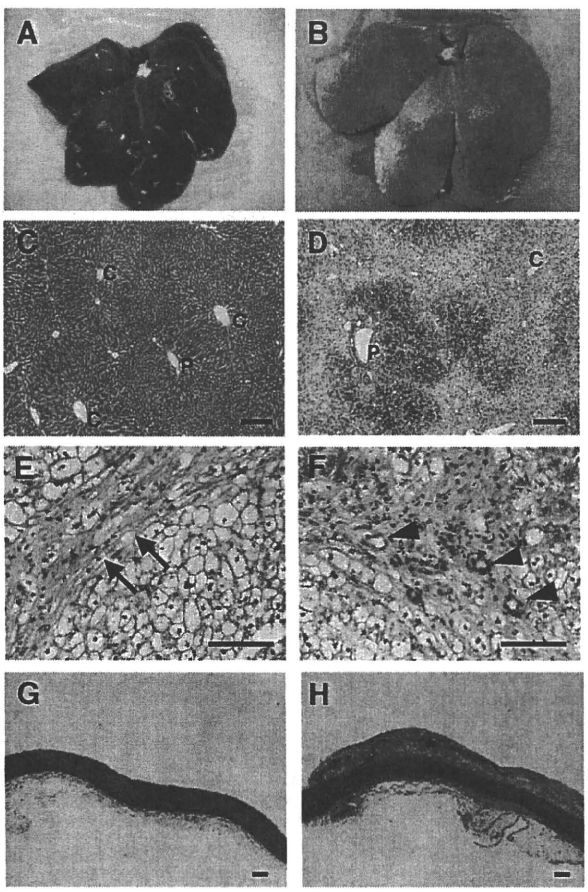

Figure 2. Steatosis and fibrosis in the liver of HFD II-fed rabbits. Rabbits were fed SD (**A**, **C**, and **G**) or HFD II (**B**, **D**, **E**, **F**, and **H**) for nine months. **A** and **B:** Macroscopic appearance of the livers of SD- and HFD II-fed rabbits. **C–H:** H&E staining of the liver (**C–F**) and aorta (**G** and **H**). Note that lipid-induced hepatic degeneration and liver fibrosis are predominantly seen in the livers (**D–F**) and that atheroma developed in the aorta (**H**) of HFD II-fed rabbits. **Arrows** in **E**, **arrowheads** in **F**, and **asterisk** in **H** indicate fibrotic septa, bile duct proliferation, and atheroma, respectively. P, portal vein; C, central vein. Scale bars = 100 μm.

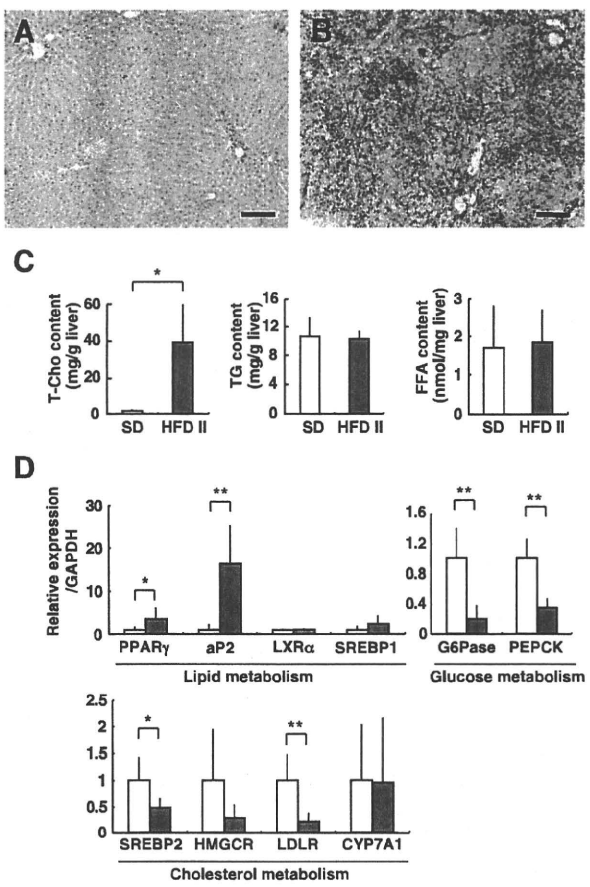

Figure 3. Metabolism of lipid, glucose, and cholesterol in the livers of HFD II-fed rabbits. Rabbits were fed SD (**A**) or HFD II (**B**) for nine months. **A** and **B:** Oil red O staining. Note hepatic lipid deposits in HFD II-fed rabbits. Scale bars = 100 μm. **C:** Hepatic T-Cho (**left**), TG (**middle**), and FFA (**right**) contents. Note that the hepatic T-Cho content increased significantly in HFD II-fed rabbits. **D:** Expression of lipid, glucose, and cholesterol metabolism-related genes in the livers of SD-fed rabbits (white bars) and HFD II-fed rabbits (gray bars) analyzed by quantitative real-time PCR. $^{*}P < 0.05$; $^{**}P < 0.01$.

in rabbits fed HFD II, whereas glucose 6-phosphatase (G6Pase) and phosphoenolpyruvate carboxykinase (PEPCK), which are involved in glucose metabolism, were reduced in the livers of HFD II-fed rabbits (Figure 3D). Among cholesterol biosynthesis-related genes, expression of sterol regulatory element binding protein 2 (SREBP2) and low-density lipoprotein receptor (LDLR) was significantly reduced in the livers of HFD II-fed rabbits. Expression of 3-hydroxy-3-methylglutaryl-coenzyme A reductase (HMGCR) mRNA also tended to be reduced in livers, although not significantly. Cytochrome P450 7A1 (CYP7A1) mRNA levels remained unchanged.

Hepatic Inflammation and Kupffer Cell Activation

RAM-11, an antibody directed against rabbit macrophages, recognizes activated Kupffer cells, the resident liver macrophages.[21] In contrast to the livers of SD-fed rabbits (Figure 4A), in the livers of HFD II-fed rabbits, the number of RAM-11-positive (RAM-11$^+$) cells increased drastically around the central vein area at sites where fatty degeneration of hepatocytes was evident (Figure 4B, see also Figure 2D). At a higher magnification (Figure 4B, inset), large RAM-11$^+$ cells were localized in sinusoids, and they frequently contained vacuoles. In accordance with this observation, genes related to macrophage activation and cytokines, such as tumor necrosis factor α (TNFα); interleukin-1β (IL-1β), -10 (IL10), and -18 (IL18); Toll-like receptors 2 (TLR2) and 4 (TLR4); CD14 (a coreceptor with TLR 4); and MD2 (a complex with TLR4), were all induced in the livers of HFD II-fed rabbits (Figure 4C, Supplemental Table S2, see *http://ajp.amjpathol.org*).

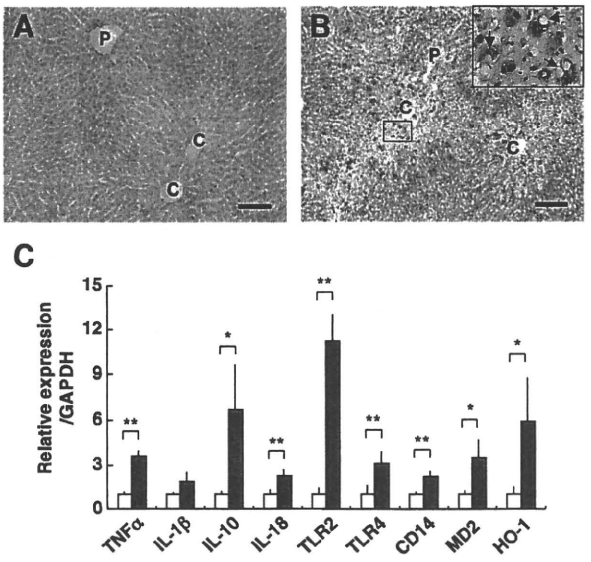

Figure 4. Activation of macrophages in the livers of HFD II-fed rabbits. Rabbits were fed SD (**A**) or HFD II (**B**) for nine months. **A** and **B:** Immunohistochemistry for the rabbit macrophage RAM-11 clone. Note RAM-11$^+$ cells around the central vein area in HFD II-fed rabbits, whereas these cells are absent in SD-fed rabbits. **Inset:** enlarged view of the box. **Arrows** indicate RAM-11$^+$ cells with large vacuoles. Scale bars = 100 μm. P, portal vein; C, central vein. **C:** Expression of inflammatory genes in the livers of SD-fed rabbits (white bars) and HFD II-fed rabbits (gray bars) analyzed by quantitative real-time PCR. $^*P < 0.05$; $^{**}P < 0.01$.

A stress protein, heme oxygenase-1 (*HO-1*), was also increased significantly in the livers of HFD II-fed rabbits.

Advanced Hepatic Fibrosis in Rabbits Fed High-Fat and -Cholesterol Diet II

The livers of HFD II-fed rabbits showed evidence of advanced fibrosis. Sirius red staining showed a limited amount of red-colored collagen around portal and central veins in the control livers, whereas collagen deposition was marked in the livers of HFD II-fed rabbits (Figure 5, A and B). Fibrosis formed bridges between the central veins and central portal veins, indicating that the liver fibrosis was stage 3 (bridging fibrosis) or stage 4 (cirrhosis) according to the Brunt's staging score. The fibrotic septa were composed of cells positive for αSMA, a marker of activated stellate cells and myofibroblasts (Figure 5, C and D). Up-regulated expression of αSMA in HFD II-fed rabbits was confirmed by immunoblotting (Figure 5E). In addition, expression of genes associated with fibrosis, such as transforming growth factor β1 (TGFβ1), collagens 1A1 (Col1A1) and 3A1 (Col3A1), matrix metalloproteinases-2 (MMP-2) and -9 (MMP-9), and tissue inhibitors of metalloproteinases-1 (TIMP-1) and -2 (TIMP-2), increased in the livers of HFD II-fed rabbits (Figure 5F, Supplemental Table S2, see *http://ajp.amjpathol.org*). Furthermore, genes for other matrix proteins such as

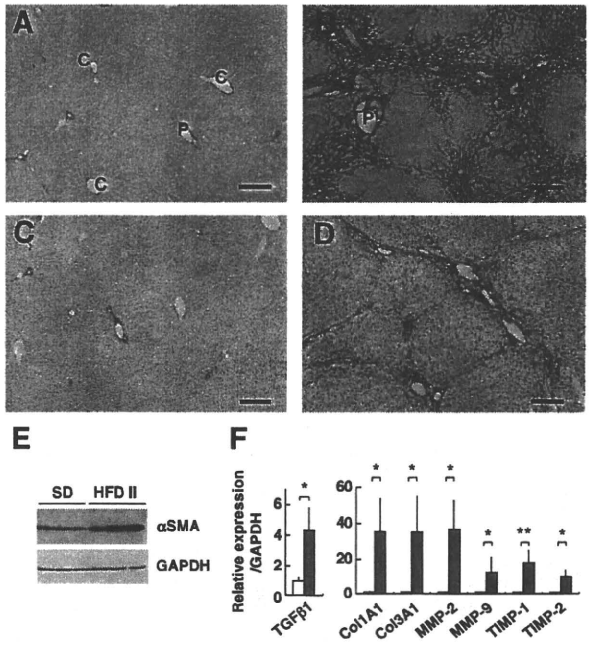

Figure 5. Progression of liver fibrosis in HFD II-fed rabbits. Rabbits were fed SD (**A** and **C**) or HFD II (**B** and **D**) for nine months. **A** and **B:** Sirius red staining. Note collagen deposits around the portal and central vein areas, as well as bridging fibrosis in HFD II-fed rabbits. P, portal vein; C, central vein. **C** and **D:** Immunohistochemistry for αSMA, a marker of activated stellate cells and myofibroblasts. Note that αSMA$^+$ cells are mainly seen inside fibrotic septa in the livers of HFD II-fed rabbits. Scale bar = 100 μm. **E:** Immunoblotting for αSMA. Note that expression of αSMA was augmented in HFD II-fed rabbits. GAPDH was the internal control. **F:** Expression of fibrosis-related genes in the livers of SD-fed rabbits (white bars) and HFD II-fed rabbits (gray bars) analyzed by quantitative real-time PCR. $^*P < 0.05$; $^{**}P < 0.01$.

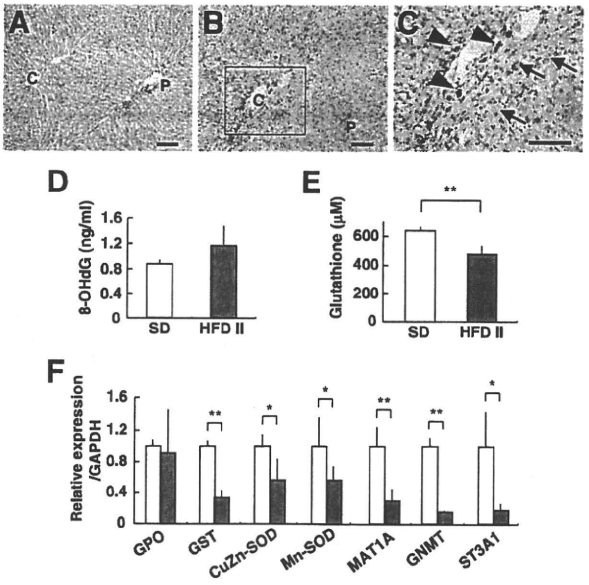

Figure 6. Detection of oxidative stress and levels of antioxidants in the liver. Rabbits were fed SD (**A**) or HFD II (**B** and **C**) for nine months. **A–C:** Staining of 4-HNE adducts in the liver. **C:** A magnified image of the region enclosed within the **box** in **B**. Note 4-HNE adducts in the hepatocytes (**arrows**) and sinusoidal cells (**arrowheads**) of HFD II-fed rabbits. Scale bars = 100 μm. **D:** Hepatic 8-hydroxy-2′-deoxyguanosine content. **E:** Glutathione content in the livers of SD- and HFD II-fed rabbits. **F:** Expression of mRNAs for antioxidant-related genes and proteome analysis of liver proteins in SD-fed rabbits (white bars) and HFD II-fed rabbits (gray bars). $^{*}P < 0.05$; $^{**}P < 0.01$.

collagen 8A1, MMP-12, TIMP-3, lumican, decorin, and biglycan showed increased expression in the livers of HFD II-fed rabbits (Supplemental Table S2, see *http://ajp.amjpathol.org*).

Oxidative Stress and Antioxidant Imbalance in Rabbits Fed High-Fat and -Cholesterol Diet II

Immunohistochemical analysis showed that 4-HNE adduct formation was rare in SD-fed rabbits but was prominent in HFD II-fed rabbits. The 4-HNE adducts were present in the cytoplasm of sinusoidal cells and hepatocytes around the central vein areas (Figure 6, A–C), indicating increased lipid peroxidation in HFD II-fed rabbit livers as in human NASH.[22] Moreover, the 8-hydroxy-2′-deoxyguanosine level increased, although not significantly, in both liver tissue and urine of HFD II-fed rabbits (Figure 6D, Table 3). As a measure of the presence of oxidative stress, the hepatic level of glutathione was determined in SD- and HFD II-fed rabbits; HFD II significantly reduced its levels (Figure 6E). In addition, the expression of genes for glutathione *S*-transferase (GST) and other antioxidant molecules, such as Cu,Zn-superoxide dismutase (Cu,Zn-SOD) and Mn-superoxide dismutase (Mn-SOD), decreased significantly in HFD II-fed rabbits (Figure 6F, Supplemental Table S2, see *http://ajp.amjpathol.org*). We measured the serum or urine levels of molecules that reflect oxidative stress. The levels of copper, δ-tocopherol, and coenzyme Q10 (ubiquinol and ubiquinone) increased significantly in HFD II-fed rabbits, whereas folic acid and vitamin A decreased significantly (Table 3). Comparison of hepatic protein distribution profiles on two-dimensional SDS-PAGE gels between SD- and HFD II-fed rabbits revealed proteins that were both up- and down-regulated by HFD II (Figure 7). GST was identified as a markedly down-regulated protein in HFD II-fed rabbits. Other down-regulated proteins in HFD II-fed rabbits by proteome analysis were glycine *N*-methyltransferase (GNMT), methionine adenosyltransferase 1 (MAT1), and sulfotransferase 3A1 (ST3A1). These genes also showed significantly lower expression in the livers of HFD II-fed rabbits (Figure 6F).

Effect of Ezetimibe on the Rabbit NASH Model

To further evaluate the rabbit NASH model, we investigated the effect of a known compound that suppresses the occurrence of NASH through a known mechanism.

Table 3. Profile of Oxidative Stress Markers and Antioxidants in Serum and Urine

	SD	HFD II	Source	*P* value
Oxidative stress				
8-OHdG (ng/mg creatinine)	43.0 ± 37.7	101.1 ± 34.6	Urine	NS
Isoplastane (ng/mg creatinine)	4.0 ± 5.3	18.2 ± 24.8	Urine	NS
Lipid peroxide (nmol/ml)	2.5 ± 1.0	3.7 ± 0.4	Serum	NS
Antioxidants				
Iron (μg/dl)	142.8 ± 65.7	115.9 ± 24.5	Serum	NS
Copper (μg/dl)	46.8 ± 2.9	156.3 ± 5.9	Serum	$P < 0.01$
STAS (μM)	969.0 ± 39.8	958.7 ± 143.5	Serum	NS
Aqueous antioxidants				
Vitamin C (μg/ml)	3.9 ± 1.3	6.3 ± 2.9	Serum	NS
Folic acid (ng/ml)	55.8 ± 11.6	21.3 ± 12.5	Serum	$P < 0.05$
Liposoluble antioxidants				
Vitamin A (μg/dl)	92.3 ± 5.1	37.6 ± 6.7	Serum	$P < 0.01$
Vitamin E fraction				
α-Tocopherol (μg/dl)	95.0 ± 81.4	3499.7 ± 5040.3	Serum	NS
δ-Tocopherol (μg/dl)	<2.5	31.2 ± 10.4	Serum	$P < 0.05$
γ-Tocopherol (μg/dl)	6.5 ± 2.7	706.9 ± 944.2	Serum	NS
Coenzyme Q10				
Ubiquinol (nmol/L)	58.0 ± 10.8	489.3 ± 151.3	Serum	$P < 0.05$
Ubiquinone (nmol/L)	N.D.	36.7 ± 23.7	Serum	$P < 0.01$

NS, not significant.

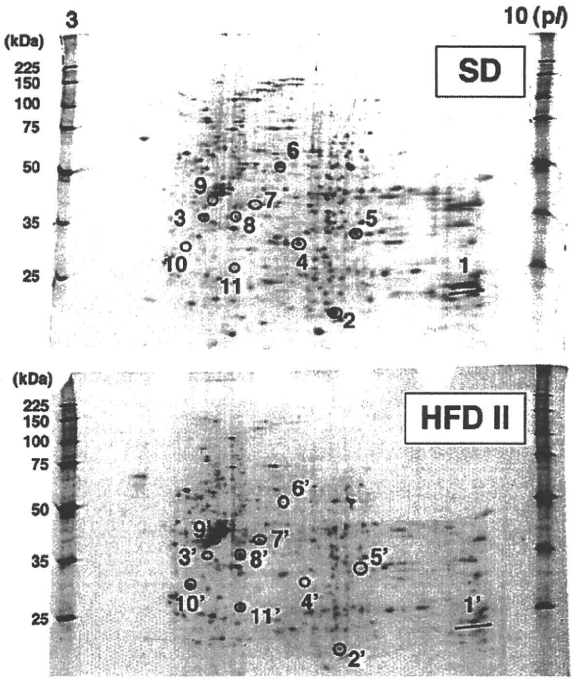

Figure 7. Two-dimensional SDS-PAGE analysis of hepatic proteins. Rabbits were fed SD or HFD II for nine months. Proteins were extracted from the livers of SD- and HFD II-fed rabbits and were separated by two-dimensional SDS-PAGE. After the gels were stained with SYPRO Ruby, the protein spots were cut out, digested, and analyzed by quadrupole time-of-flight. Then, the proteins were identified from the obtained amino acid sequences using protein BLAST or FASTA databases. 1 and 1′, glutathione transferase; 2 and 2′, glutathione *S*-transferase Yc (α II); 3 and 3′, MAT1; 4 and 4′, ST3A1; 5 and 5′, GNMT; 6 and 6′, aldehyde dehydrogenase, mitochondrial (ALDH class 2); 7 and 7′, keratin, type II or cytoskeletal 2 epidermal; 8 and 8′, α-tubulin, actin, β-like 2, or similar to actin, cytoplasmic 1; 9 and 9′, actin, β-like 2; 10 and 10′, keratin 10 or CYP2B3; 11 and 11′, similar to actin, cytoplasmic 1. Blue circles, proteins down-regulated in HFD II-fed rabbits; red circles, proteins up-regulated in HFD II-fed rabbits.

Because a marked increase in serum and hepatic T-Cho levels was evident in our HFD-fed rabbits, we tested ezetimibe, a relatively new compound that inhibits NPC1L1 in hepatocytes and the intestine. Rabbits were fed HFD I (the original diet) with or without ezetimibe (0.6 mg/kg/day) for 2 months. Both control and experimental rabbits showed normal increases in body weight (data not shown). Levels of AST, ALT, and TG remained within the normal range in rabbits fed HFD I with or without ezetimibe (AST, 38.0 ± 18.4 versus 20.8 ± 7.4 IU/L; ALT, 11.0 ± 1.0 versus 7.8 ± 3.0 IU/L; and TG, 31.0 ± 9.5 versus 27.4 ± 16.8 mg/dl). Serum T-Cho was significantly lower in HFD I-fed rabbits treated with ezetimibe than in untreated rabbits during the course of ezetimibe-treatment for up to 8 weeks (Figure 8A). A histological examination showed that ezetimibe suppressed fat deposition (Figure 8, B–F) and reduced the hepatic content of total T-Cho and TG (Figure 8G). Furthermore, liver fibrosis, mildly induced in this 2-month HFD I model, was suppressed by the ezetimibe treatment (Figure 9, A–D). Moreover, ezetimibe significantly decreased the expression of genes associated with liver fibrosis, such as TGFβ1, MMP-9, and TIMP-1 and -2. The drug also suppressed expression of Col1A1 and MMP-2, although the difference was not significant (Figure 9E).

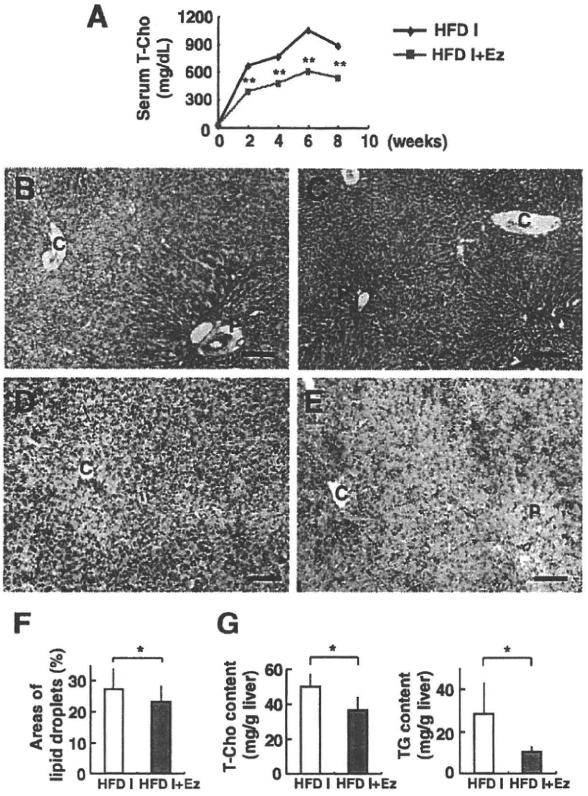

Figure 8. Effect of ezetimibe (Ez) on hepatic steatosis in HFD I-fed rabbits. Rabbits were fed HFD I (the original diet) with or without ezetimibe (0.6 mg/kg/day) (HFD I or HFD I + Ez) for two months. Histological sections were prepared from HFD I-fed (**B** and **D**) and HFD I + Ez-fed rabbits (**C** and **E**). **A:** Changes in serum T-Cho levels. **B** and **C:** H&E staining. **D** and **E:** Oil red O staining. Scale bars = 100 μm. **F:** Quantification of the lipid droplet area in the liver. Oil red O-stained areas were measured in the livers of HFD I- and HFD I + Ez-fed rabbits. The stained area was significantly smaller in HFD I + Ez-fed rabbits. **G:** Hepatic total cholesterol and triglyceride contents. P, portal vein; C, central vein. HFD I, $n = 5$. HFD I + Ez, $n = 5$. $^{*}P < 0.05$; $^{**}P < 0.01$.

Discussion

There are several important differences in characteristics of NASH between this rabbit model and humans. Hepatic levels of cholesterol, but not of TG and FFA, exhibited a marked increase in HFD II-fed rabbits compared with those in SD-fed rabbits, and the PPARγ and aP2 mRNA levels were induced in the HFD II model in a manner similar to that observed in human NASH (Figure 3, C and D).[26,27] NAFLD shows various patterns of lipid deposition in the liver,[28] which may be influenced by the diet composition. In this context, increased PPARγ and aP2 may contribute to a decrease in cholesterol level in hepatocytes of this rabbit model induced by high-cholesterol diets. Mitochondrial free cholesterol, but not TG and FFA, sensitizes hepatocytes to TNFα- and Fas-induced apoptosis through mitochondrial glutathione exhaustion.[29] We also observed a marked reduction in glutathione and glutathione-metabolic enzymes in the HFD II-fed rabbit livers (Figure 6, E and F). In this context, it is likely that cholesterol overload, together with a dysregulated antioxidative system in hepatocytes, may trigger liver injury.[30,31] Furthermore, this rabbit model showed increased levels

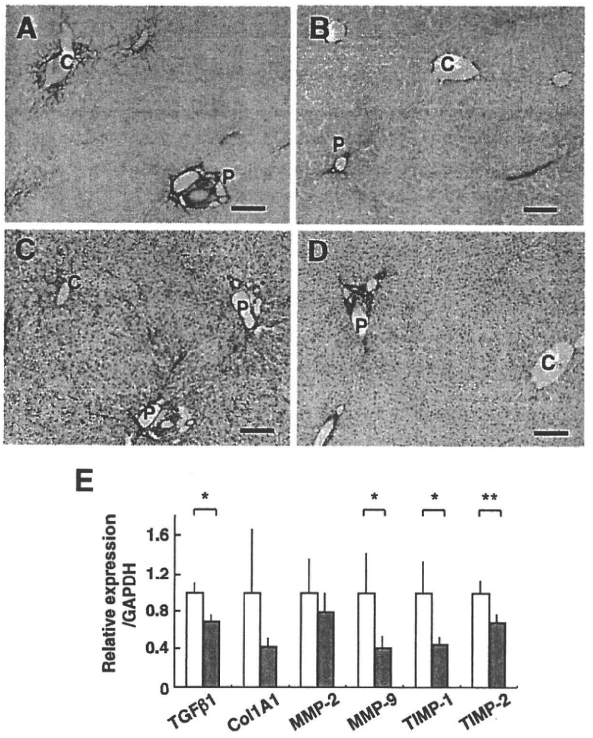

Figure 9. Effect of ezetimibe (Ez) on liver fibrosis in HFD I-fed rabbits. Rabbits were fed HFD I (the original diet) with or without ezetimibe (0.6 mg/kg/day) (HFD I or HFD I + Ez) for two months as mentioned in Figure 8. Histological sections were prepared from HFD I-fed (**A** and **C**) and HFD I + Ez-fed rabbits (**B** and **D**). **A** and **B:** Liver sections were stained with Sirius red. Collagen depositions were reduced by ezetimibe administration. **C** and **D:** Liver sections were immunostained for αSMA. Note that the αSMA^+ cells were reduced by ezetimibe administration. Scale bars = 100 μm. **E:** Expression of fibrosis-related genes in the liver of HFD I-fed rabbits (white bars) and HFD I + Ez-fed rabbits (gray bars). P, portal vein; C, central vein. HFD I, $n = 5$. HFD I + Ez, $n = 5$. Ez, ezetimibe. $^*P < 0.05$; $^{**}P < 0.01$.

of serum bile acids (Table 2), which are presumably induced by cholesterol overload and down-regulation of the bile acid export-related genes, such as the bile salt export pump and multidrug resistance-associated protein 2 (data not shown).

Although it has been reported that FFA and leptin increase and adiponectin decreases in the serum of NASH patients,[32] serum and hepatic levels of FFA did not change in this rabbit model, possibly owing to the lack of obesity. A recent study reported the reduction of serum adiponectin in a rabbit model fed 10% lard and 2% cholesterol-containing HFD for 8 and 12 weeks.[33] Unfortunately, we were unable to determine the adiponectin and leptin levels in our rabbit model for unknown reasons (data not shown).

We also observed no increase in fasting glucose, fasting insulin, or HOMA-IR in this rabbit model. However, as stated above, this rabbit model showed no obesity and failed to induce high FFA levels in the liver and serum, which may be reasons for its failure to induce type II diabetes and insulin resistance. Furthermore, as shown in Figure 3D, G6Pase and PEPCK mRNA expression levels were markedly suppressed in the HFD II model, similar to a report on cirrhotic NASH patients.[34] Cholesterol overload and the resulting hepatocyte dysfunction in cirrhosis are assumed to be the reasons for this down-regulation, indicating the actual impairment of glucose metabolism in the HFD II liver.

The serum ALT level has long been used as a surrogate marker for liver injury. However, ALT values do not correlate well with the severity of liver injury in human NAFLD.[35,36] Similar to that in patients with NAFLD but that inunlike viral or drug-induced hepatitis, the ALT level in this rabbit model remained unchanged, but the mechanism remains unknown and should be clarified in future research.

Gut-derived lipopolysaccharide activates Kupffer cells by activating lipopolysaccharide receptors,[37] leading to increased production of inflammatory cytokines such as TNFα, IL-8, and IL-18.[38,39] The development of steatohepatitis in a NASH model, induced by a methionine- and choline-deficient diet, was partly inhibited in TLR4 mutant mice,[40,41] suggesting a role for TLR4-dependent signaling in the occurrence of this type of liver damage. In addition, the lipoprotein component of endotoxin from Gram-negative and -positive bacteria activates TLR2 and/or TLR4, which leads to common downstream activation of TRAF6 via the adapter molecule MyD88.[42] This cascade of events culminates in nuclear factor-κB activation, leading to the induction of TNFα and other proinflammatory cytokines.[42] Although TNFα has been identified as a central mediator contributing to insulin resistance and liver damage in NASH, little is known about the role of TLR2 or TLR4 in the induction of TNFα. In the present study, we observed an increase in the expression of TLR4/CD14/MD2 and TLR2 and cytokine induction in HFD II-fed rabbits. Persistent hepatic inflammation also triggers the activation of stellate cells and excess collagen production, resulting in the development of liver fibrosis.[43,44] Stellate cells are activated by LPS through TLR4/CD14/MD2 signaling.[45,46] Thus, the role of LPS in triggering steatohepatitis in this HFD II model deserves to be studied further in relation to hepatic fibrogenesis.

In the present study, we showed a reduction in hepatic glutathione content and decreased GST and SOD mRNA expression. Serum levels of antioxidants such as vitamin E, copper, and coenzyme Q10 increased significantly, but the levels of vitamin A and folic acid decreased significantly. As a result, there was an imbalance between oxidative stress and antioxidant protection systems in the present steatohepatitis model, as in human NASH patients.[47–52] The molecular mechanisms leading to the dysregulation of small antioxidant molecules are currently unknown. Most vitamin A in the body (approximately 70%) is usually stored in quiescent hepatic stellate cells,[53] but vitamin A storage is impeded when stellate cells are activated, under which activation they express αSMA and produce extracellular matrix materials including type I collagen.[43,44] Thus, the reduction of serum vitamin A levels may reflect activation of stellate cells and the progression of fibrosis in our rabbits with HFD II-induced NASH. Folic acid is reportedly involved in the maintenance of normal concentrations of homocysteine, methionine, and *S*-adenosylmethionine.[54] Folic acid deficiency and abnormal hepatic methionine metabolism